Supplementary Information for:

From binary AB to ternary ABC supraparticles

*E. Deniz Eren[1], Mohammad-Amin Moradi[1], Mark M. J. van Rijt[1], Bernette M. Oosterlaken[1], Heiner Friedrich[1,2] and Gijsbertus de With[1]**

[1] *Laboratory of Physical Chemistry and Center for Multiscale Electron Microscopy, Department of Chemical Engineering and Chemistry, Eindhoven University of Technology, Eindhoven, The Netherlands*

[2] *Institute for Complex Molecular Systems, Eindhoven University of Technology, Eindhoven, The Netherlands*

[] *Present address: Department of Chemistry, McGill University, 801 Sherbrooke Street West, Montreal, Quebec H3A 0B8, Canada*

Keywords: Supraparticles, Colloidal Self-assembly, Silica Nanoparticles, Iron oxide Nanoparticles, Polystyrene Nanoparticles, CryoTEM

**Correspondence to:* G. de With (G.deWith@tue.nl; orcid.org/0000-0002-7163-8429)

Experimental

Materials and Methods

Polystyrene latex nanoparticles*, *Iron oxide (II, III) nanoparticles and Titanium dioxide powder

Aqueous suspensions of Polystyrene latex (PSL) nanoparticles (NPs) were obtained from either Sigma-Aldrich (LB1) or Fisher Scientific (Distrilab) and used as received. Polystyrene latex nanoparticles (Aldrich) with a diameter of 80 nm, 100 nm, 140 nm, 170 nm and 450 nm containing 0.1% Sodium Azide preservative and a trace amount of surfactant were used for size effect experiments. Aqueous suspensions of Magnetite (Fe_3O_4) nanoparticles (NPs) with diameter of 30 nm were obtained from Sigma-Aldrich (CAS No. 1317-61-9). Titania nanoparticles (TiO_2) powder with diameter of 30 nm was obtained from Nanoshel (CAS No. 13463-67-7).

Synthesis and Surface Modification of Silica Nanoparticles

Synthesis of silica nanoparticles with controlled sizes was achieved using the Yokoi method [1] in combination with a method reported by Carcouët *et al*. [2] that uses lysine (Fluka) in combination with tetraethyl ortho silicate (TEOS, VWR). Following the Yokoi method, 100 mg L-lysine was dissolved in 100 ml pure water in a three-neck 250 ml flask and the reaction mixture was magnetically stirred at 270 rpm under reflux at 60 °C. Thereafter, the reaction was initiated by adding tetraethyl orthosilicate (TEOS) (6 ml for 30 nm silica nanoparticles and

0.6 ml for 10 nm silica nanoparticles) in one swift motion to the reaction solution. The reaction was continued for 24 h, followed by size measurement on the resulting particles by Dynamic Light Scattering (DLS, ZetaNano) and cryoTEM imaging (Supplementary Information 1 (SI1), Figure S1). The diameter of as-synthesized SiO_2 NPs used to form supraparticles in this study was measured to be 28 ± 0.9 nm (SI1, Figure S2) and 24 ± 1.2 nm (SI1, Figure S3), respectively. The sizes of the SiO_2 NPs are reported as mean ± standard deviation of the mean.

Functionalization of the surface of silica nanoparticles with amine groups was performed based on the method described by Pham *et al*. [3] using (3-Aminopropyl) triethoxysilane (APTES, Sigma-Aldrich, CAS Number 919-30-2), with a 1:50 – 1:200 weight ratio of APTES to silica. APTES was diluted in THF to a 4% (V/V) APTES in THF solution. The desired amount of the APTES-THF solution was pipetted into a stirring sample of silica dispersion, after which stirring was continued vigorously for 30 minutes.

Formation of AB Supraparticles using Polystyrene and Silica Nanoparticles

For assembly experiments a stock dispersion was prepared by diluting the PSL NPs dispersion 1:10 with water. The buffer volume added was calculated based on the desired ionic strength for the specific sample volume (see table S1). The remaining sample volume was thereafter split between a PSL stock dispersion and a (modified) silica dispersion to a V_{silica}/V_{PSL} = 0.8 ratio (Number of PSL NPs in the solution is 9.14×10^{11}, while number of SiO_2 NPs in the solution is 5.48×10^{13}). To investigate the influence of the size ratio of particles on the ordering of small nanoparticles on larger ones, we used different sizes of large and small nanoparticles. For silica particles with a diameter between 20 nm to 30 nm and for polystyrene particles with a diameter between 80 nm to 450 nm were chosen.

Formation of ABC Supraparticles using Polystyrene, Silica and Magnetite nanoparticles

Depending on the inorganic nanoparticles that were employed, two different assembly procedures were followed to create ABC supraparticles. For supraparticles consisting of 10 nm and 30 nm SiO_2 NPs, a stock dispersion was prepared by diluting the PSL NPs dispersion 1:10 with water, followed by addition of APTES modified 30 nm SiO_2 NPs ($V_{30nmsilica}/V_{PSL}$ = 0.4 ratio, number of PSL NPs in the solution kept the same 9.14×10^{11}, while number of SiO_2 NPs in the solution is halved 2.74×10^{13}) to ensure the formation of stable, partially covered supraparticles. Thereafter, the APTES modified 10 nm SiO_2 NPs were mixed with the stable partially covered supraparticles to a $V_{10nmsilica}/V_{mixture}$ = 0.32 ratio (here, the number of partly

covered supraparticles equals to the initial number of PSL NPs in the solution which is 9.14×10^{11}. Thereafter, the calculation of the number of 10 nm SiO_2 NPs is done by considering the number of partly covered supraparticles in the solution. As we were able to predict the number of 10 nm SiO_2 NPs needed to cover a large nanoparticle by using the formula proposed by Mansfield et al., we adjusted the number of 10 nm SiO_2 NPs to 8.98×10^{13}) to initiate the formation of ABC supraparticles.

To create ABC supraparticles consisting of 10 nm SiO_2 NPs and 30 nm Fe_3O_4 NPs, as a first step concentration of Fe_3O_4 stock solution was increased by a factor of 14 using an Amicon Ultra centrifugal ultrafiltration unit (Millipore Sigma, SKU number UFC501008). Thereafter a stock dispersion was prepared by diluting the PSL NPs dispersion 1:10 with water, followed by the addition of 30 nm Fe_3O_4 NPs to a $V_{30nmFe3O4}/V_{PSL}$ = 0.4 ratio (the number of PSL NPs in the solution kept the same as 9.14×10^{11}, while number of Fe_3O_4 NPs in the solution in the solution is adjusted to 2.74×10^{13}) to create stable partially covered supraparticles with a sufficient number of Fe_3O_4 particles attaching the surface of the PSL NPs. Finally, the APTES modified 10 nm SiO_2 NPs were mixed with the stable partially covered supraparticles to a $V_{10nmsilica}/V_{mixture}$ = 0.32 ratio (at this point, as the most important parameter is the size ratio between nano building blocks, the number of nanoparticles (A as PSL NPs, B as 30 nm Fe_3O_4, and C as 10 nm SiO_2 NPs) in our system is kept same as prior system where we formed ternary ABC supraparticles) to initiate the formation of ABC supraparticles.

CryoTEM Sample Preparation

CryoTEM studies were performed on the TU/e cryoTITAN (Thermo Fisher Scientific, www.cryotem.nl) equipped with a field emission gun (FEG), a post-column Gatan Energy Filter (model 2002) and a post-GIF 2k × 2k Gatan CCD camera (model 794). Data were acquired at 300 kV acceleration voltage. Samples were prepared by depositing 3 µl samples on a 200 mesh Cu grid with a Quantifoil R 2/2 holey carbon film (Quantifoil Micro Tools GmbH) or Lacey / Carbon 200 mesh (Electron Microscopy Sciences). All TEM grids were surface plasma treated for 40 s using a Cressington 208 carbon coater prior to use. An automated vitrification robot (Thermo Fisher Scientific, Vitrobot Mark IV) was used for plunge vitrification in liquid ethane. Images were recorded with a total electron flux of less than 100 $e^{-}\cdot Å^{-2}$. In-house Matlab scripts were used for TEM image analysis.

Cryo-electron Tomography

Cryo-electron micrographs of the tomography tilt series were acquired by tilting the specimen from −68° to 68° with 2° increments. The cryo-TEM images are taken at 6500-, 11500- and 19000-times magnification, corresponding to a pixel size of 1.4, 0.76 and 0.47 nm. Nominal defocus values used were –10, –5, and –2 µm, respectively. The total dose for one tilt-series is about 400 $e^{-}.Å^{-2}$. Tomographic tilt series acquisition was performed with Inspect 3D software (Thermo Fisher Scientific). Alignment (using SiO_2 NPs as the markers or patch tracking modules) and reconstruction were carried out in IMOD, either using SIRT with 5-20 iterations[4] or using back projection. Subsequently, in some cases, data were denoised by a nonlinear anisotropic diffusion filter or a median filtering with a 3x3 kernel size prior to visualization. For all measurements a beam-damage-avoiding protocol was used (see SI2). The resulted 3D reconstructions are shown in the supplementary movies (SM) SM1 – SM16.

SI 1: Characterization of the organic and inorganic building blocks

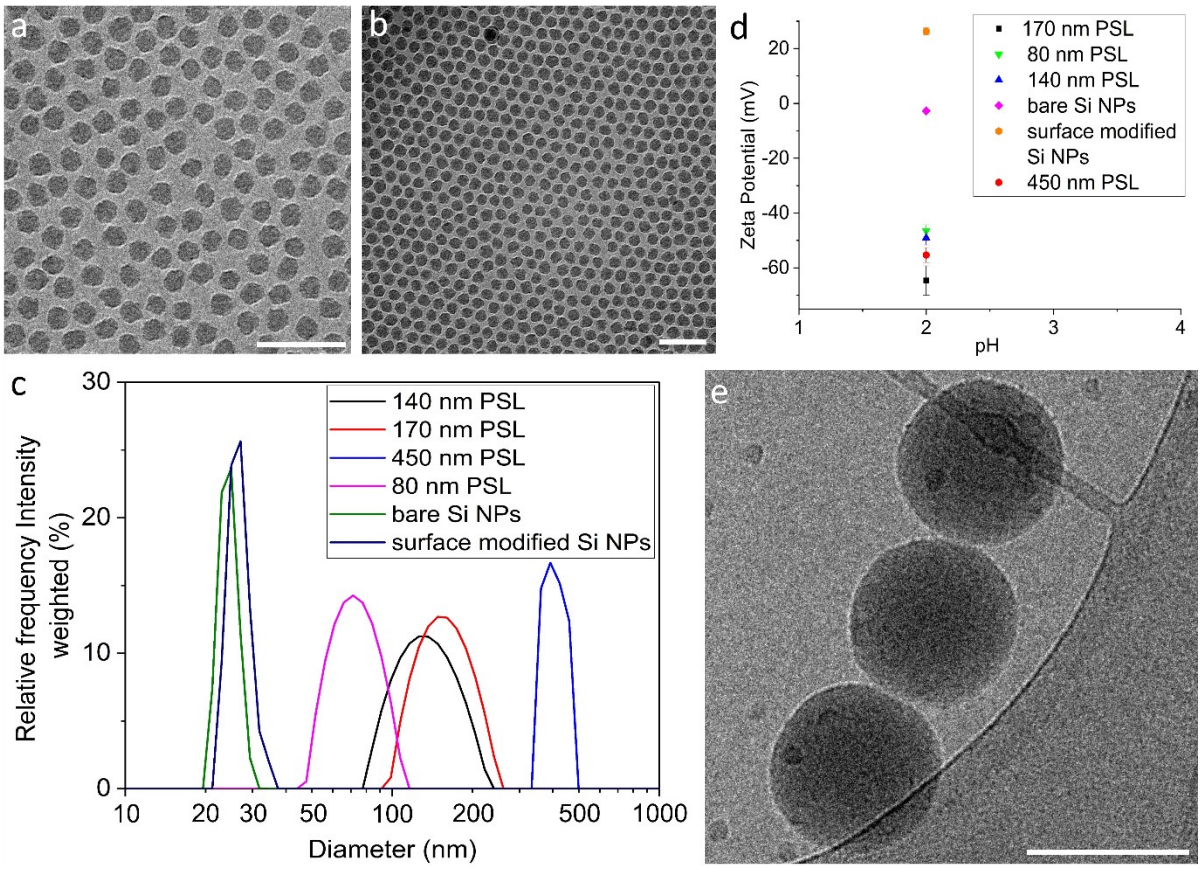

Figure S1. Characterization of the organic and inorganic nanoparticles used in this study*: CryoTEM image of a), b) the as-synthesized silica nanoparticles, c) the DLS results of the different nanoparticles used in this study, d) the surface charge of the polystyrene latex nanoparticles, as-synthesized and*

surface-modified silica nanoparticles, and e) a representative cryoTEM image of the polystyrene latex nanoparticles. Scale bars: 100 nm.

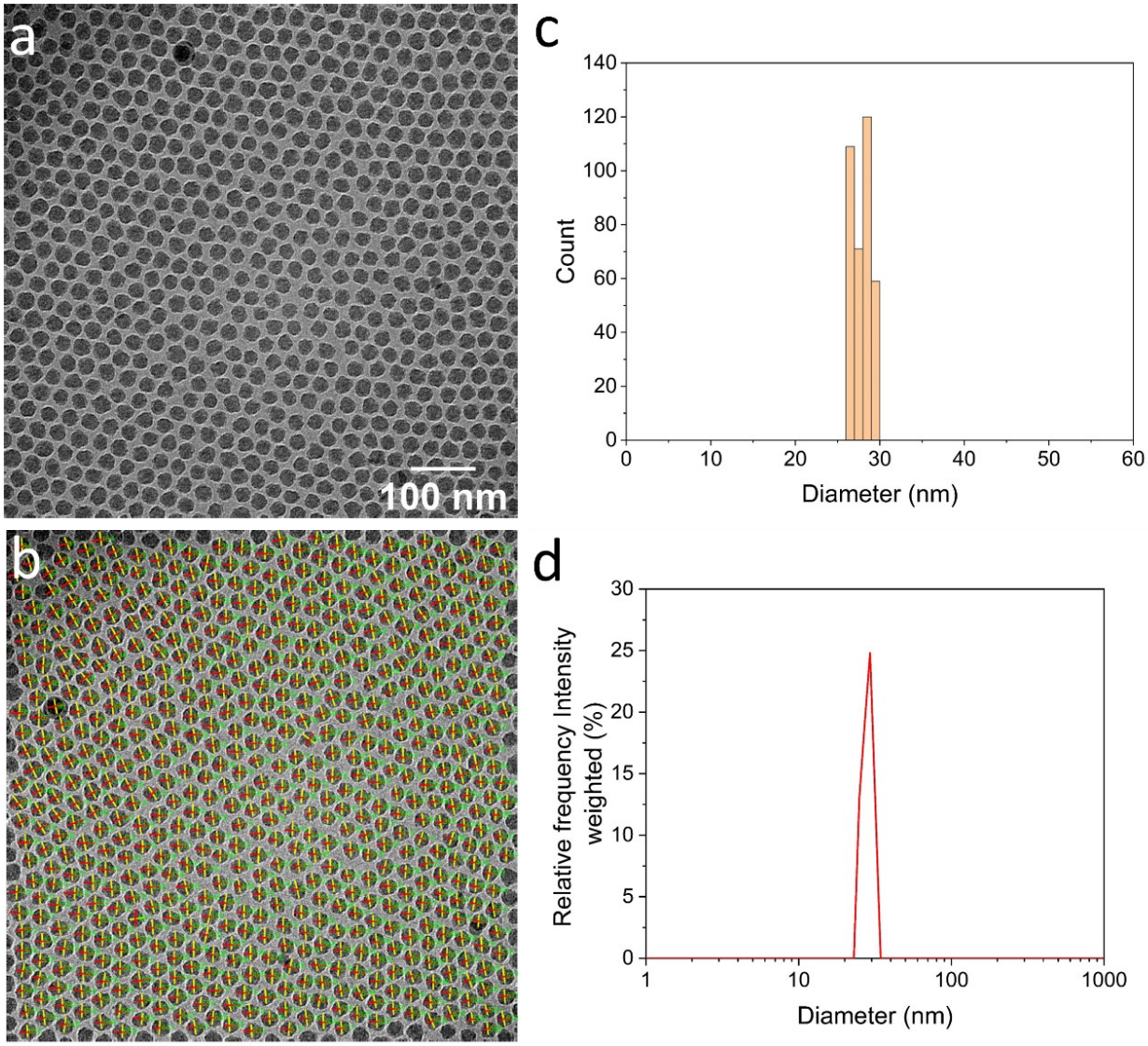

Figure S2. *The size distribution of the SiO_2 NPs determined from a-b) cryoTEM images using an in-house made MATLAB script, c) Histogram showing the size distribution of silica nanoparticles obtained from image b, and d) The number distribution of the size of the silica nanoparticles determined by DLS.*

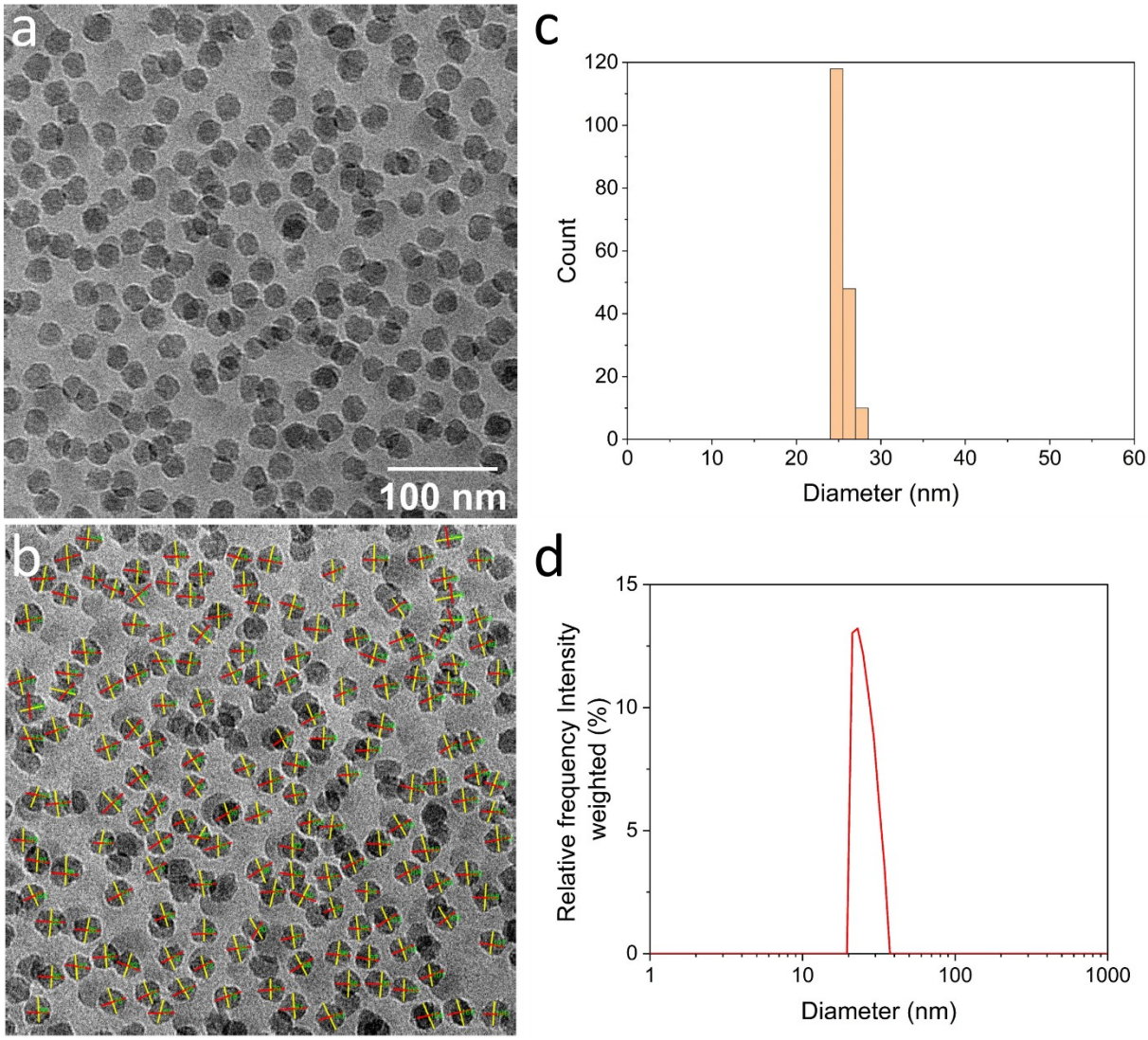

Figure S3. *The size distribution of the SiO_2 NPs determined from a-b) cryoTEM images using an in-house made MATLAB script, c) Histogram showing the size distribution of silica nanoparticles obtained from image b, and d) The number distribution of the size of the silica nanoparticles determined by DLS.*

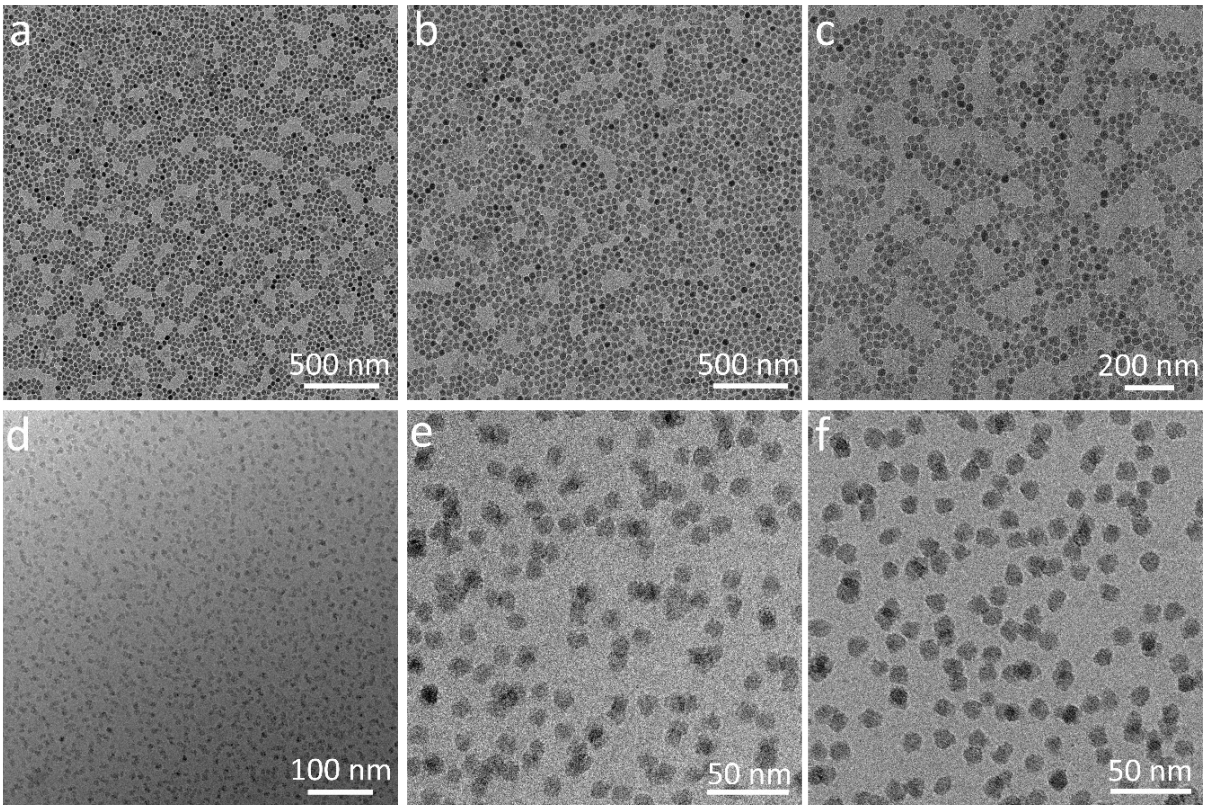

Figure S4 Characterization of two different inorganic building blocks used to create ternary ABC supraparticles*: TEM images of a-c) 30 nm Fe_3O_4 nanoparticles and d-f) CryoTEM images of 10 nm SiO_2 nanoparticles.*

SI 2: Cryo-electron tomography procedure

Prior to conducting electron tomography procedure, the maximum electron dose which can be applied to either the AB or ABC supraparticles before beam damage on the structures can be observed, was determined by acquiring 100 images, with an electron dose of 4 $e^{-}Å^{-2}$ per image resulting in a cumulative dose of 400 $e^{-}Å^{-2}$. Four sets of 100 images were acquired on two different spots of the sample containing ABC supraparticles which were created either by using 10 nm and 30 nm SiO_2 or 10 nm SiO_2 and 30 nm Fe_3O_4 particles Beam damage was not observed on any of the particles in these regions. Therefore, it was decided to perform the tilt series by acquiring 67 images at 4 $e^{-}Å^{-2}$ per image resulting in a cumulative dose of 268 $e^{-}Å^{-2}$, well below the highest investigated cumulative dose.

SI 3: Surface modification of silica nanoparticles

The SiO_2 NPs used in this study were surface modified with (3-Aminopropyl) triethoxysilane (APTS or APTES) by using a protocol described by Pham et al.[3] in order to add amino groups to

the surface of SiO_2 NPs. In order to successfully modify the surface of SiO_2 NPs, initially, APTES was diluted in Tetrahydrofuran (THF) to a 4% (V/V) (or 4.2% (m/m)) APTES to THF solution. Thereafter, surface modified SiO_2 NPs were made by adding 10 µl of 4% (V/V) THF to 2.35 ml bare SiO_2 NPs which resulted in a surface modified SiO_2 with a weight ratio of 1:50 of silane to silica. Owing to the high reactivity[5] of APTES in water, it is expected that no free silane remains in the solution which was also demonstrated by Pham et al.[3] and Kaiser et al.[6]. Moreover, it was demonstrated that, when added to water, the triethoxysilane groups hydrolyze to form silanols in the solutions[5]. Through the condensation reaction of silanols, these hydrogen bonds are converted into covalent links forming a network of polymers. Thereafter, these networks of polymers deposit on the surface of SiO_2 NPs and bind to them via further condensation reaction for which an illustration is shown in Figure S3.

Owing to the condensation mechanism shown above, the silanes cannot form a single layer on the surface of silica, but rather form a multilayer. The size difference that we observed in our study (~ 3 nm) after the surface modification of SiO_2 is attributed to this particular effect. It was demonstrated in the literature that the size of the APTES molecule is 1.5 nm[7]. Munguía-Cortés et al. showed the surface modification of SBA-15 with APTES and measured the reduction in pore size after the surface modification. They found a pore size reduction of 4 nm[7] comparing the surface-modified and bare samples. Moreover, by using a similar approach Jung et al.[8] modified the surface of silica nanoparticles in order to determine the effectivity of different surface modification procedures. They found that, while the diameter of bare silica nanoparticles was 137 nm, it was changed to 141 nm after the surface modification as demonstrated by using DLS and TEM.

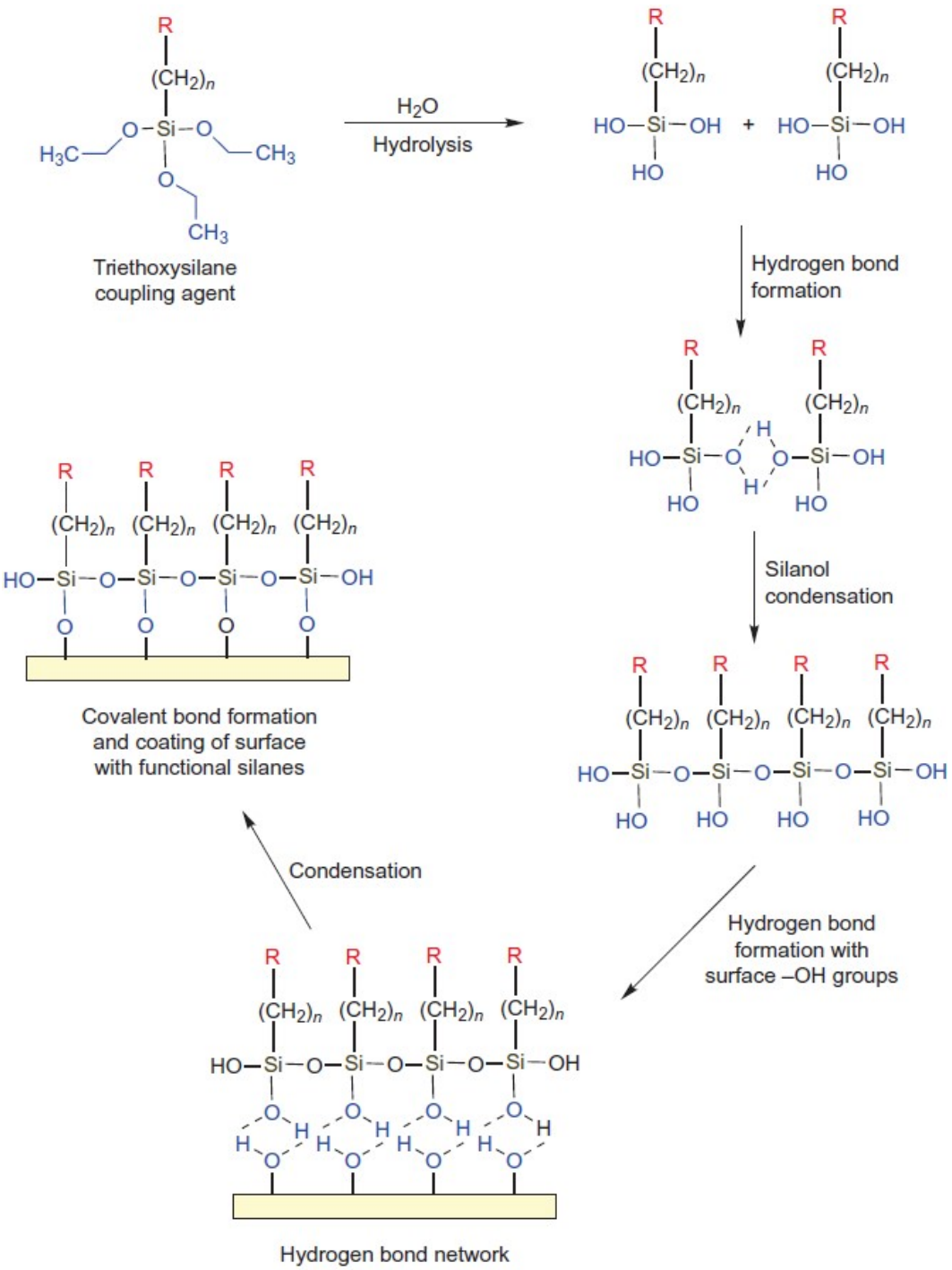

Figure S5. *Reaction path of APTES with the surface of SiO_2 NPs in the aqueous medium (Adapted with permission from ref [5]).*

SI 4: Partially covered binary AB supraparticles

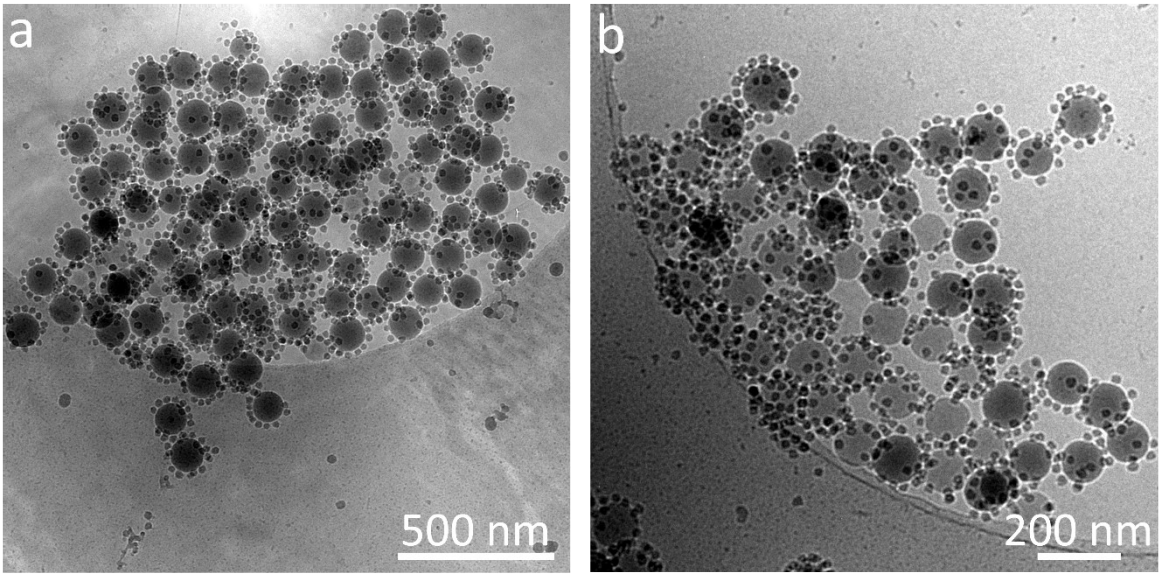

Figure S6 . *CryoTEM results of mixture where partial coverage of PSL NPs by SiO_2 NPs can be seen due to the low concentration of SiO_2 NPs.*

SI 5: SEM and TEM characterization of the 30 nm TiO_2 and 10 nm Fe_3O_4 nanoparticles

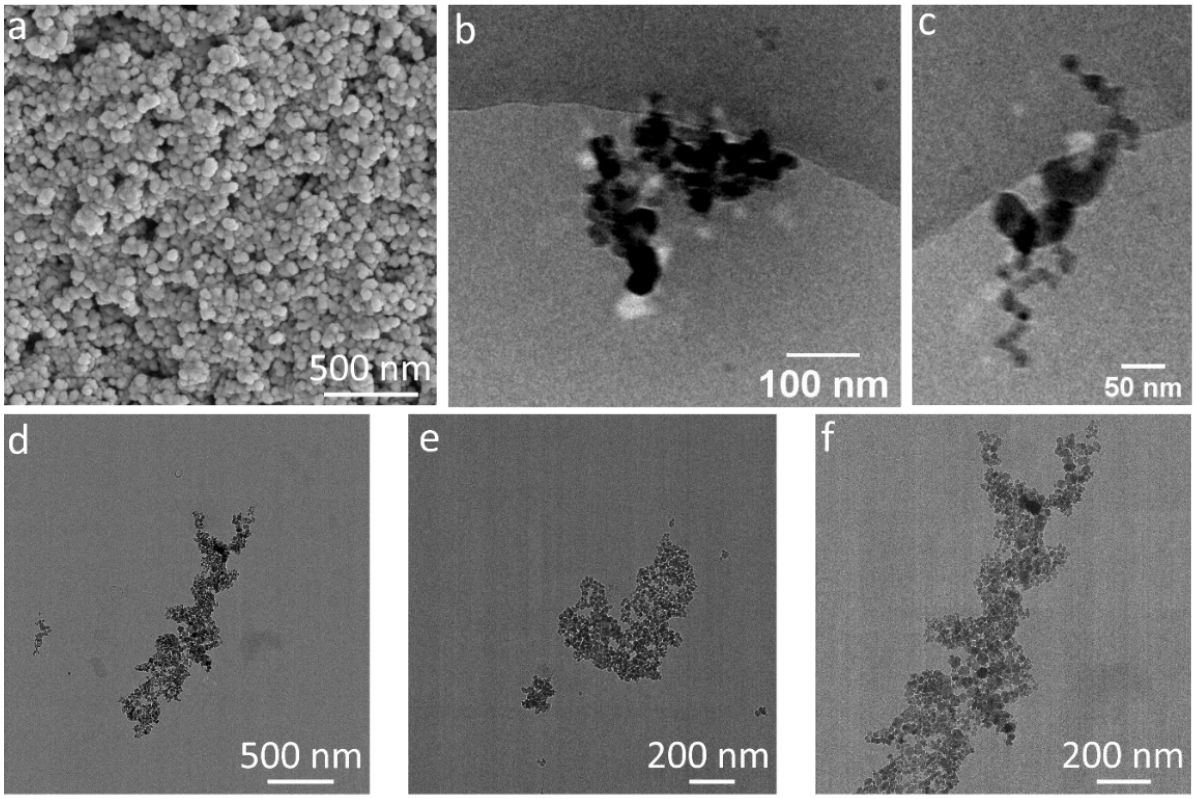

Figure S7: Characterization of the different inorganic nanoparticles used in this study*: SEM image of a) titanium nanoparticles, b,c) CryoTEM images of the same titanium nanoparticles, d) Representative TEM images of 10 nm Fe_3O_4 nanoparticles.*

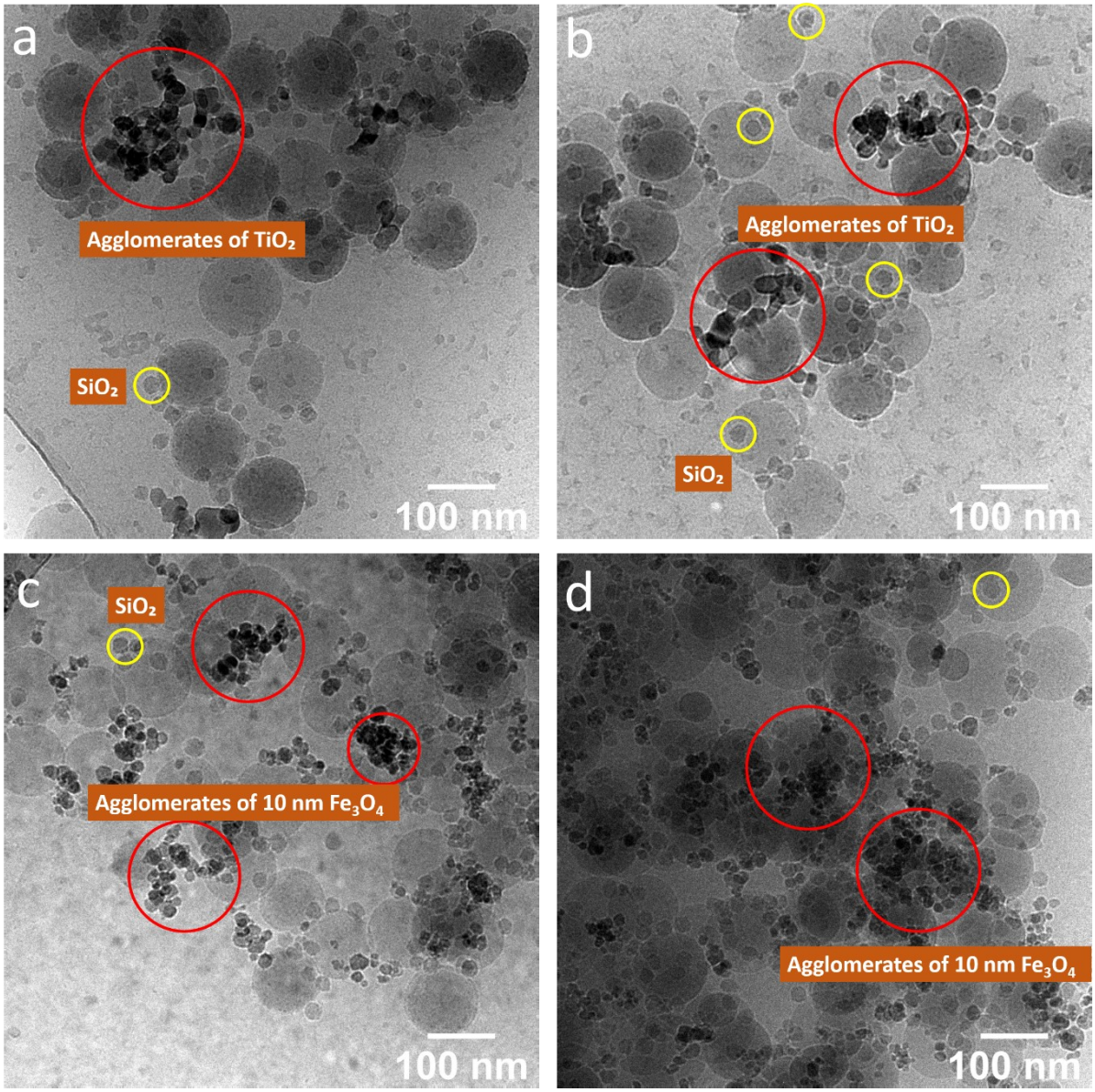

Figure S8. Characterization of the unsuccessful attempts to form ternary ABC supraparticles*: CryoTEM images of partially covered binary AB supraparticles and a), b) agglomerated 30 nm TiO_2 nanoparticles and c), d) agglomerated 10 nm SiO_2 nanoparticles.*

SI 6: Stable partially covered binary AB supraparticles with different surface charge densities

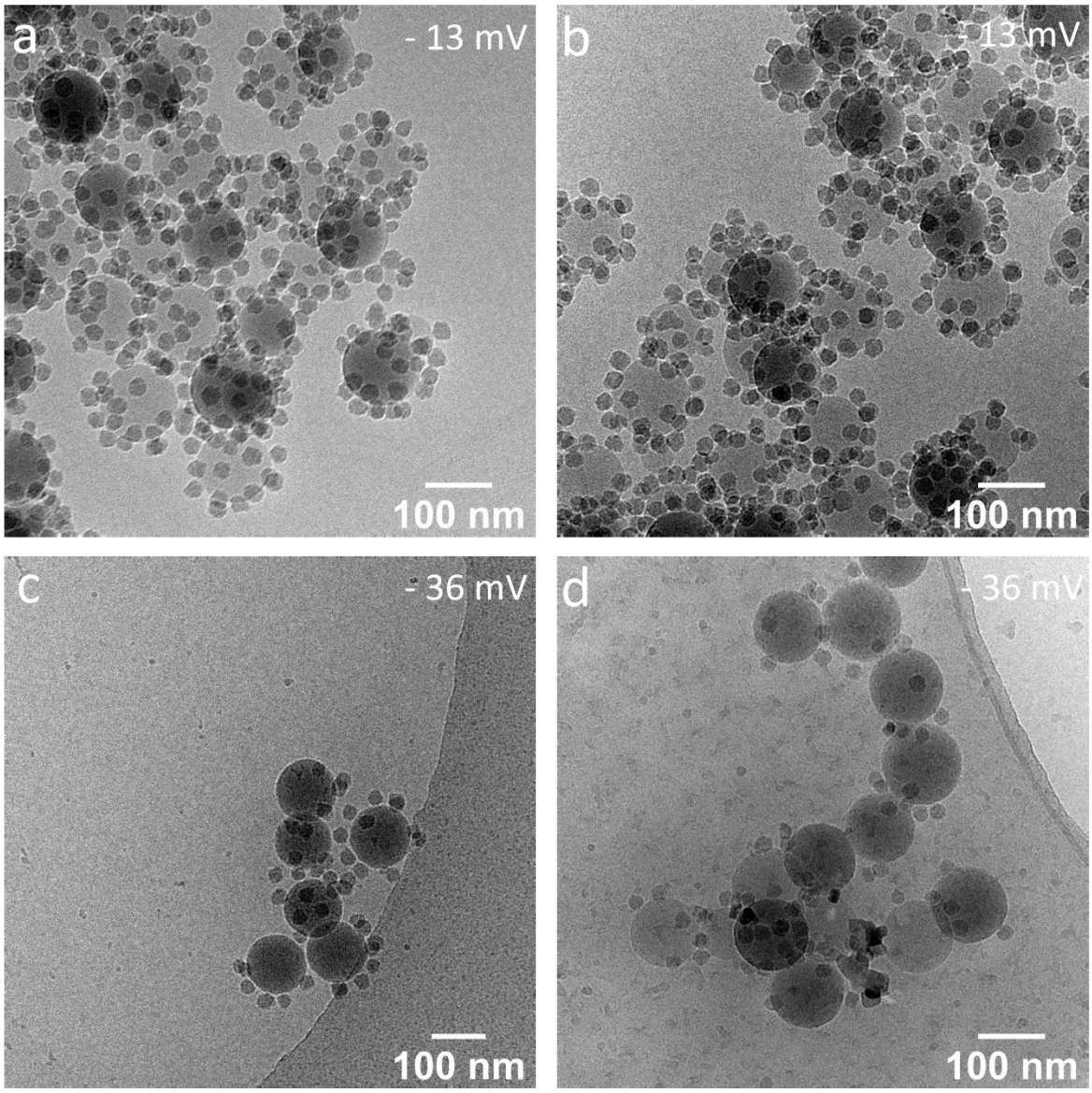

Figure S9 Characterization of partially covered AB supraparticles*: CryoTEM images of partially covered binary AB supraparticles a), b) with a zeta potential value of –13 mV and c), d) with a zeta potential value of –36 mV.*

SI 8: Stability of ternary ABC supraparticles using 10 nm and 30 nm SiO_2 nanoparticles

Here we employ Derjaguin-Landau-Verwey-Overbeek (DLVO) theory to determine the colloidal stability of the individual inorganic nanoparticles, the polystyrene latex nanoparticles and the supraparticles which are formed by utilizing different inorganic nanoparticles. According to the DLVO theory, the net interaction between two nanoparticles (VDLVO) is the sum of the repulsive electrostatic double-layer or Coulomb interactions (V_{Coul}) and the attractive van der Waals (V_{vdW}) interaction potential, so that

$$V_{DLVO} = V_{vdW} + V_{Coul}$$

The Poisson-Boltzmann equation is used to calculate the electrostatic interactions between two spherical objects of equal surface potential and equal size. The classical DLVO theory is based on the linearized Poisson-Boltzmann equation for which an analytical solution exists, but various approximate expressions for the non-linear case have been proposed. Similar as in our recent publication [9], here we also used the expression as given by Sader et al. [10] in order to calculate the electrostatic interaction potential between two spherical objects at the constant surface potential for any distance regardless of the particle size:

$$V_{Coul} = 64\pi\left(\frac{R^2}{2R+h}\right)\varepsilon_r\varepsilon_0\left(\frac{k_BT}{ze}\right)^2 Y^2 \ln\left(1 + exp(-\kappa h)\right) \quad \text{where}$$

$$Y = exp(\kappa h/2)\tan^{-1} h\left(exp(-kh/2)\tan h\left(\psi_0/4\right)\right)$$

with e (C) being the elementary charge, ε_0 (F·m^{-1}) the vacuum permittivity, ε_r (-) the permittivity (dielectric constant) of the medium, k_B (J·K^{-1}) the Boltzmann constant and T (K) the temperature. Further, h the closest separation between the nanoparticles' surfaces, ψ_0 the surface potential of the particle of interest (which can be an individual nanoparticle system or supraparticles), z is the valency, and κ the Debye length. The latter is given by:

$$\kappa^2 = 2e^2 I/\varepsilon_r\varepsilon_0 kT$$

The equations mentioned above are suitable approximations for the numerical calculations of the full Poisson-Boltzmann equation at a constant surface potential.

The van der Waals attraction between two supraparticles of equal size is calculated according to the Hamaker formulation of intermolecular forces assuming pairwise additivity. Although this is an approximation, it nevertheless describes the physical origin of the interaction well.

The expression for the van der Waals interaction potential [11] is given by:

$$V_{vdW} = -\frac{A_H}{6}\left[\frac{2R^2}{h^2+4Rh}+\frac{2R^2}{h^2+4Rh+4R^2}+\ln\left(\frac{h^2+4Rh}{h^2+4Rh+4R^2}\right)\right]$$

where R is the radius of the particle, h is the closest distance between the surface of nanoparticles, and A_H is the Hamaker constant, which quantifies the properties of the material. For the calculation, we consider one single supraparticle as a particle composed of a spherical polystyrene latex core and either iron or silica nanoparticles attached to the curved surface. The radius of iron and silica nanoparticles used was either $R_{Silica} \cong 15$ nm and $R_{Iron} \cong 15$ or $R_{Silica} \cong 5$ nm, while polystyrene latex core radius was $R_{PS} \cong 50$ nm which totals to a nano-raspberry nanoparticle diameter of either D = 160 nm or D = 120 nm. For iron oxide (F), silica (S), and polystyrene (P) A_H values as given by Bergström [12], A_H(F)= 4.6×10^{-21} J, A_H(S)= 4.6×10^{-21} J, and by Tsaur [13] and Fowkes [14], A_H(P)= 5.0×10^{-21} J were used. For supraparticles covered with either Fe_3O_4 or SiO_2 nanoparticles, the values $A_H = 2.4\times10^{-20}$ J and $A_H = 4.6\times10^{-21}$ J were used, respectively.

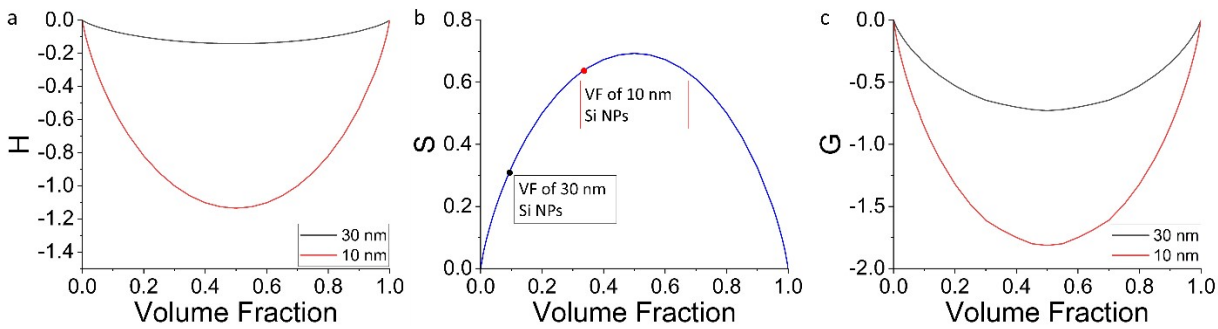

Figure S10 *(a) The enthalpy of mixing H = $\Delta_{mix}H/kT$ for 30 and 10 nm Si NPs; (b) The entropy of mixing S = $\Delta_{mix}S/k$; (c) The Gibbs energy of mixing G = $\Delta_{mix}G/kT$ for 30 and 10 nm SiO_2 NPs at constant pressure in kT units per particle as a function of volume fraction of the components present in the ternary system.*

From thermodynamics models for polymer blends and dissolved polymers, it is possible to calculate the thermodynamic conditions such as temperature, pressure, and composition under which phase separation occurs. Whether two polymers are mutually miscible or a polymer is soluble in a solvent depends on the sign of the Gibbs energy which is related to the enthalpy and entropy of mixing. At thermodynamic equilibrium, self-assembly evolves the components of a system into a structure that corresponds to the minimum of the appropriate

thermodynamic potential. This potential is determined by the thermodynamic parameters that are held constant during the process. For example, if the temperature (T), pressure (P), and the number of molecules (N) in the system stay constant, self-assembly tends to minimize the Gibbs energy:

$$G_{mix} = H_{mix} - T\,S_{mix}$$

where H is the enthalpy and S is the entropy, and whose changes, $\Delta_{mix}G = \Delta_{mix}H - T\,\Delta_{mix}S$, determine the spontaneity of the process: the reaction is spontaneous if $\Delta_{mix}G < 0$.

In our study, the formation of ABC supraparticles is fundamentally a displacement reaction where 10 nm SiO_2 NPs replace the 30 nm SiO_2 NPs which are located on the surface of the PSL NPs. Written as a quasi-chemical reaction, we have

$$PS_x^{30} + y(S^{10}) \rightarrow PS_y^{10} + x(S^{30})$$

where PS_x^{30} represents a PSL NP covered with x SiO_2 NPs with size 30 nm, y the number of 10 nm SiO_2 NPs labeled S^{10} initially floating free in the solution necessary to cover the PS core, PS_y^{10} a PSL NP covered with y NPs with size 10 nm SiO_2, x the number of 30 nm Si NPs floating free in the solution after they have replaced the 10 nm SiO_2 NPs. We define the number density (or concentration) as

$$n = N/V$$

where N is the total number of nanoparticles in interest (either the 10 nm and 30 nm SiO_2 NPs or the 100 nm PSL NPs) in a volume V. In our ternary system, where free 10 nm SiO_2 NPs have the ability to replace 30 nm SiO_2 NPs, the number density of 10 nm SiO_2 NPs, 30 nm SiNPs, and 100 nm PSL NPs are 1.57×10^{11}, 2.27×10^{10}, and 3.73×10^{9} m^{-3}, respectively. According to our CryoTEM results, upon adding 30 nm SiO_2 NPs to create partially covered supraparticles, all PSL NPs are partially covered and no naked PSL NPs are present in our system which means that the number density of partially covered supraparticles is equal to the number density of PSL NPs in the system. Moreover, as we did not observe any free 30 nm SiO_2 NPs in the solution coexisting with partially covered supraparticles, it is reasonable to assume that all 30 nm SiO_2 NPs are used. Furthermore, 10 nm SiO_2 NPs were added to the system with partially covered supraparticles present in order to initiate the formation of ternary ABC supraparticles. We assume that we can estimate the enthalpy of the supraparticles as the sum of the binary

energies for the invidual inorganic particles on the PS core, so that the enthalpy change becomes

$$\Delta H = H(PS_y^{10}) - H(PS_x^{30}) \text{ with } H(PS_y^{10}) = yU_{DLVO}(PS^{10}) \text{ and } H(PS_x^{30}) = xU_{DLVO}(PS^{30})$$

For the entropy of the S^{10} and S^{30} particles we use the Flory-Huggins expression

$$S = \phi \ln\phi + (1-\phi) \ln(1-\phi)$$

dependent on their volume fraction $\phi(S^{10})$ or $\phi(S^{30})$, so that the entropy change becomes

$$\Delta S = S(S^{30}) - S(S^{10})$$

Considering ΔG overall, but neglecting the entropy for PS^{30} and PS^{10} as they provide a small contribution, we finally have

$$\Delta G = G(PS_y^{10}) + xG(S^{30}) - G(PS_x^{30}) - yG(S^{10})$$

To estimate the thermodynamic stability, we need some numbers. Experimentally it appears that the maximum number of 30 nm SiO_2 NPs on a 100 nm PS is approximately 60 and the maximum number of 10 nm SiO_2 NPs on a 100 nm PS is approximately 260. Based on experimental observations, we assume that after partial coverage with 30 nm SiNPs, the number of 30 nm SiO_2 NPs on a 100 nm PS is approximately 30 and that the after partial coverage with 10 nm SiO_2 NPs, the number of 10 nm SiO_2 NPs on a 100 nm PS is approximately 130. The enthalpy ($H = \Delta_{mix}H/kT$) is calculated using DLVO theory and leads a binary enthalpy of PS and 30 nm SiO_2 NPs of -0.15 kT (reactant side) and a binary enthalpy of PS and 10 nm SiO_2 NPs of -1.13 RT (product side). The entropy ($S = \Delta_{mix}S/k$) of mixing the 60 SiO_2 of size 30 nm (0.12) that go in solution is 0.36 k, while the mixing entropy of the 260 SiO_2 of size 10 nm (0.32) that go in solution is 0.62 k. Therefore the Gibbs energy ($G = \Delta_{mix}G/kT$) becomes $G_{10\text{ nm SiNPs}} = -1.75$ kT and $G_{30\text{ nm SiNPs}} = -0.51$ kT. The results are plotted in Figure S10. Both the PS^{30} and PS^{10} supraparticles are stable but upon adding the 10 nm SiO_2 NPs to partially covered PS^{30} supraparticles, the stability of the system increases rendering the creation of ternary ABC supraparticles possible. The reverse is clearly not possible (Figure S11).

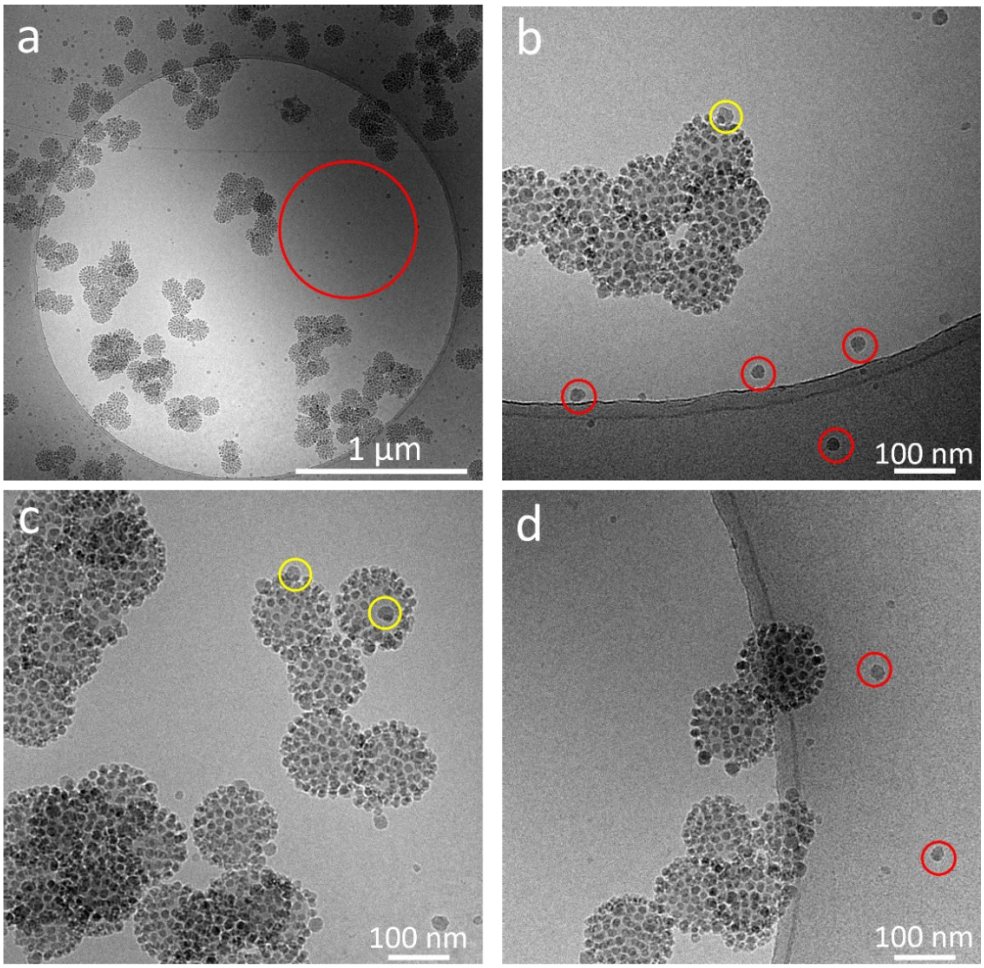

Figure S11 Characterization of ternary ABC supraparticles*: CryoTEM images of ternary ABC supraparticles created by using 10 nm and 30 nm SiO_2 and 100 nm PSL NPs. Red circles indicate free 30 nm SiO_2 nanoparticles, while yellow circles indicate a few of the 30 nm SiO_2 NPs which were able to attach the surface of binary AB supraparticles.*

SI 9: Stable partially covered AB supraparticles using Fe_3O_4 as initial building block

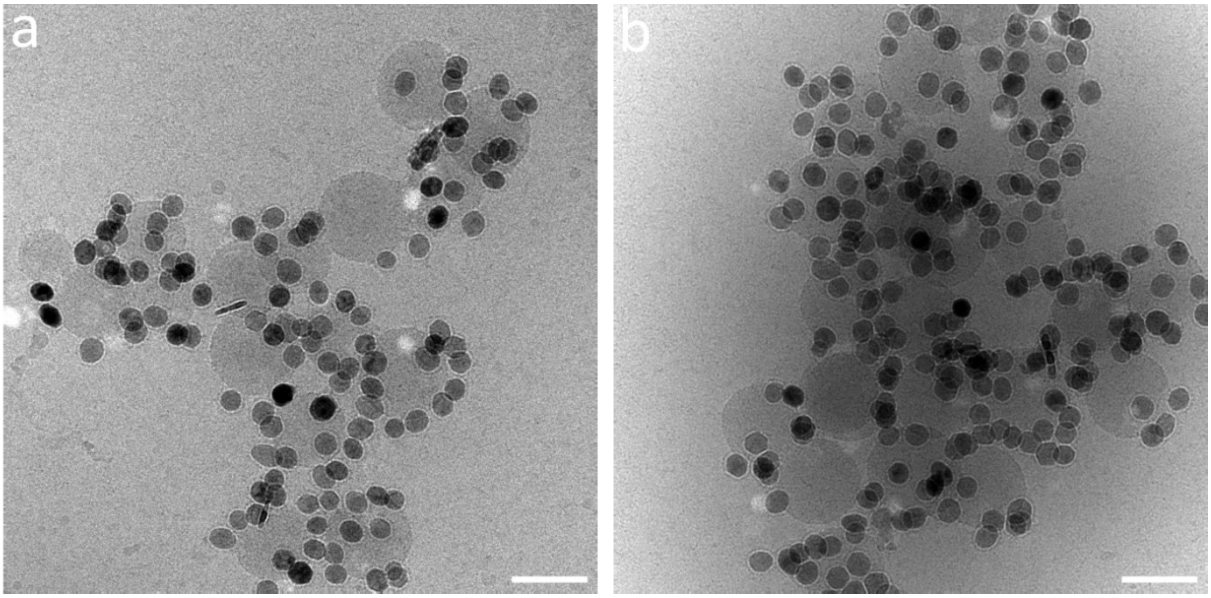

Figure S12 Characterization of partially covered AB supraparticles*: CryoTEM images of partially covered binary AB supraparticles formed by using 30 nm Fe_3O_4 nanoparticles and 100 nl PSL NPs. Scale bars: 100 nm.*

E. D. Eren, M. Moradi, H. Friedrich, de With G., Building Reversible Nano-raspberries, *Nano Lett.* **21**, 2232–2239 (2021).

Supplementary Tables

Table S1. Composition of pH buffers used in this study.

Target pH	*Measured pH*	*Ingredient A*	*Concentration of A (M)*	*Volume of A (ml)*	*Ingredient B*	*Concentration of B (M)*	*Volume of B (ml)*	*Ionic Strength (mM)*
2	1.6	KCl	0.1	50	HCl	0.1	13	79.4
4	3.9	Acetic acid	0.1	164	CH_3COONa	0.1	36	72
6	5.9	KH_2PO_4	0.1	100	NaOH	0.1	11.6	89.6
12	12.4	KCl	0.1	50	NaOH	0.1	12	80.6

References

1 T. Yokoi, Y. Sakamoto, O. Terasaki, Y. Kubota, T. Okubo and T. Tatsumi, *J. Am. Chem. Soc.*, 2006, **128**, 13664–13665.
2 C. C. M. C. Carcouët, M. W. P. van de Put, B. Mezari, P. C. M. M. Magusin, J. Laven, P. H. H. Bomans, H. Friedrich, A. C. C. Esteves, N. A. J. M. Sommerdijk, R. A. T. M. van Benthem and G. de With, *Nano Lett.*, 2014, **14**, 1433–1438.
3 K. N. Pham, D. Fullston and K. Sagoe-Crentsil, *Aust. J. Chem.*, 2007, **60**, 662–666.
4 D. Chen, H. Friedrich and G. de With, *J. Phys. Chem. C*, 2014, **118**, 1248–1257.
5 G. T. Hermanson, *Bioconjugate Tech.*, 2013, 535–548.
6 P. I. Kaiser, E., Colescott, R. L., Bossinger, C. D., & Cook, *Anal. Biochem.*, 1970, **34**, 595–598.
7 L. Munguía-Cortés, I. Pérez-Hermosillo, R. Ojeda-López, J. M. Esparza-Schulz, C. Felipe-Mendoza, A. Cervantes-Uribe and A. Domínguez-Ortiz, *J. Mex. Chem. Soc.*, 2017, **61**, 273–281.
8 H. S. Jung, D. S. Moon and J. K. Lee, *J. Nanomater.*, 2012, **2012**.
9 E. D. Eren, M.A. Moradi, H. Friedrich and G. de With, *Nano Lett.*, 2021, **21**, 2232–2239.
10 J. E. Sader, S. L. Carnie and D. Y. C. Chan, *J. Colloid Interface Sci.*, 1995, **171**, 46–54.
11 W. Russel, W.B., Saville, D.A., and Schowalter, *Colloidal dispersions*, Cambridge University Press, Cambridge, 1989.
12 L. Bergström, *Adv. Colloid Interface Sci.*, 1997, **70**, 125–169.
13 S.-L. Tsaur and R. M. Fitch, *J. Colloid Interface Sci.*, 1987, **115**, 463–471.
14 F. M. Fowkes, *Ind. Eng. Chem.*, 1964, **56**, 40–52.